

PCCP

Accepted Manuscript



This is an *Accepted Manuscript*, which has been through the Royal Society of Chemistry peer review process and has been accepted for publication.

Accepted Manuscripts are published online shortly after acceptance, before technical editing, formatting and proof reading. Using this free service, authors can make their results available to the community, in citable form, before we publish the edited article. We will replace this *Accepted Manuscript* with the edited and formatted *Advance Article* as soon as it is available.

You can find more information about *Accepted Manuscripts* in the [Information for Authors](#).

Please note that technical editing may introduce minor changes to the text and/or graphics, which may alter content. The journal's standard [Terms & Conditions](#) and the [Ethical guidelines](#) still apply. In no event shall the Royal Society of Chemistry be held responsible for any errors or omissions in this *Accepted Manuscript* or any consequences arising from the use of any information it contains.

Prediction of electronic structure of single-walled black phosphorus nanotubes

Lixiu Guan,¹ Guifeng Chen,² and Junguang Tao,^{2,*}

¹*School of Science, Hebei University of Technology, Tianjin 300130, China*

²*Key Lab. for New Type of Functional Materials in Hebei Province, School of Materials Science and Engineering, Hebei University of Technology, Tianjin 300130, China*

Abstract: Due to its high carrier mobility and tunable bandgap, phosphorene has been a subject of immense interest recently. Here we show using density functional theory based calculations that black phosphorus (BP) nanotubes are achievable. The electronic properties of BP nanotubes are explored. As contrast to its monolayer and bulk counterparts, most BP nanotubes possess indirect band gaps. In addition, strong anisotropic electronic behaviors are observed between zigzag and armchair nanotubes. Semiconducting to semi-metallic transition occurs only for zigzag tubes when its diameter shrinks to ~ 1.5 nm. The difference are strongly related to the bond bending after forming the nanotubes which governs the s - p hybridization as well as electron distribution in different p orbitals that eventually determines the electronic structure of BP nanotubes.

Keywords: Black phosphorus; Nanotubes; Density functional theory (DFT)

*Email: jgtao@hebut.edu.cn

Introduction

Since the discovery of graphene, two-dimensional (2D) layered crystals with atomic thickness have drawn increased attentions in recent years that may impact future electronic technologies.¹⁻⁷ Many exotic physical and chemical phenomena emerged at monolayer limit owing to the confinement of electrons and holes within the 2D layer. Although graphene exhibit various interesting optical and electronic properties, its intrinsic zero bandgap limits its technological applications. Recently, monolayer black phosphorus (BP) or phosphorene was successfully exfoliated from its bulk form which consists of stacked puckered 2D honeycomb layers and shows excellent semiconducting performances.⁸⁻¹¹ For an isolated phosphorene the band gap is in the range of 0.8 to 1.5 eV.^{8,12} Interlayer interactions reduce the band gap for each layer added and eventually set 0.3 eV for bulk BP.^{10,13} Bulk BP shows an electron mobility of up to $\sim 10,000 \text{ cm}^2/\text{V}^{-1} \text{ s}^{-1}$ and an on/off ratio up to 10^4 was achieved for phosphorene transistors at room temperature.^{9,11-13} The outstanding electronic performances make phosphorene quickly become the subject of significant theoretical and experimental investigations.¹³⁻²⁰

For real technologies applications, modifications and engineering are generally applied to enhance the materials/devices functionalities. Especially for new materials, great efforts are needed to explore its function enhancement in all manner of possibilities. As well demonstrated for carbon families, the wrapping of

graphene can form carbon nanotubes which possess novel properties for a wide variety of applications in nanotechnology, electronics, optics and other fields of materials science. In addition, nanotubes have also been reported for various inorganic compounds such as BN,²¹ TiO₂,²² ZnO²³ and MoS₂.²⁴ In recent studies, it was found that BP can withstand a tensile strain up to 30%²⁵ due to its small Young's modulus,²⁶ which makes BP nanotubes worth of expecting. Indeed, in previous studies, BP nanotubes have been theoretically shown possible.²⁷⁻²⁹ In addition, observations of phase transition from semiconductor to metal¹² and superconductor under high pressure³⁰ indicate correlated phenomena play an important role in BP under extreme conditions. Up to date, the knowledge of the electronic properties of BP is very important which is still quite limited. In order to widen the range of applications of phosphorene, it is necessary to further explore the correlation of its structure engineering with the electronic modification.

In this work, we performed calculations based on a first-principles method to predict atomic and electronic structures of BP nanotubes. In consistent with early studies, our results suggest that the BP nanotubes are energetically achievable.^{27,28} To advance these studies, the aim of current work is to deepen the understanding of the electronic structure variation of different kinds of BP nanotubes, namely, different sized zigzag and armchair ones. It is found that semiconducting to semi-metallic transition can be obtained in zigzag nanotubes. The electronic anisotropy is

related to the s - p hybridization and p orbitals distributions especially in valley P atoms which show significant effect on the phase transition and energy gap evolution. In particular, the shift of p orbital at the bottom of conduction band are the key factors to close the gap for BP nanotube. This finding provide a new platform for low-dimensional electronics applications.

Calculation details

Our calculations are performed by using the Vienna Ab-initio Simulation Package (VASP). The valence and core interactions are treated by the projected augmented wave (PAW) method³¹ and the exchange correlation energy was described by the generalized gradient approximation (GGA).³² The Kohn-Sham orbitals were expanded in a plane-wave basis with a cutoff energy of 500 eV. The Brillouin zone (BZ) was sampled by $8 \times 1 \times 1$ ($1 \times 9 \times 1$) Monkhorst-Pack k -point grids for zigzag (armchair) nanotubes. All atoms are relaxed and the final forces exerted on each P atom are less than $0.005 \text{ eV}/\text{\AA}$. The total ground state energy is converged within 10^{-6} eV per atom.

Results and discussions

BP possesses a layered structure where each phosphorus atom is covalently bonded with three adjacent phosphorus atoms to form a highly corrugated

anisotropic honeycomb-like structure with armchair and zigzag edges,^{8,12} see the ball-and-stick model in Fig. 1(a). This structural anisotropy leads to anisotropic band structure, electrical conductivity, thermal conductivity, and optical responses. For instance, the zigzag direction hosts free carriers that behave like massive which is several times heavier than that in armchair direction. To construct single-walled BP nanotubes, the monolayer BP was wrapped along either zigzag or armchair direction. For either direction, several sized nanotubes within 1-4 nm were constructed in order to study the size effect. In Fig. 1, the representative structures of BP nanotubes are given. Similar to carbon nanotubes, they are called zigzag and armchair nanotube as shown in Fig. 1(b) and (c), respectively, according to the shape along the perimeter. In the following, the nanotubes will be denoted a pair of indices (n, m) , where integers n and m denote the number of unit vectors along zigzag and armchair directions in the crystal lattice. If $m = 0$, the nanotubes are called zigzag nanotubes, and if $n = 0$, the nanotubes are called armchair nanotubes. After forming the nanotubes, the symmetry between upper (P1 in Fig.1(a)) and lower P (valley P, P3 in Fig.1(a)) atoms are broken as well as their bonding geometry, as listed in Table I. For zigzag nanotubes, the bond length for inner P (P3) rings is slightly decreased from 2.22 Å to 2.18 Å, while that of the outer P (P1) rings is stretched to 2.52 Å. However, the change of bond lengths and angles for armchair nanotubes are almost negligible. They are 2.21 Å for inner ring and 2.24 Å for outer ring. Similar trend is

observed for the bonding angles. This suggests the armchair nanotubes would be more stable than zigzag ones. Indeed, this is corroborated by the total system energy. From the energy point of view, the formation of nanotube raise the system energy as compared to flat monolayer BP. The energy gain for $(0, 20)$, $(0, 15)$, $(0, 10)$, $(25, 0)$, $(18, 0)$ and $(10, 0)$ nanotubes are 19 meV, 30 meV, 59 meV, 87 meV, 138 meV, and 308 meV per P, respectively. At temperature of 1000 °C which is a common temperature for sample synthesis, the energy gain of 19 (308) meV, corresponds to a relative probability of the presence being as high as 84 % (6.5 %). As one can see that for armchair nanotubes, even for the smallest size studied, its relative presence probability is as high as 60%. These high predicted presence probabilities suggest that the BP nanotubes is experimental achievable especially for armchair ones. This is also in consistent with early studies.^{27,28}

To access their electronic structure, in Fig. 2, we show the calculated density of states (DOS) for all tubes. On the left panel, from Fig. 2(a) to (c), the DOS spectra for the armchair nanotubes are presented with decreasing tube size. The corresponding spectra for zigzag tubes are exhibited on the right panel, from Fig. 2(d) to (f). As seen in Fig. 2, the energy gap shrinks for smaller tubes in both types, which is similar to that of MoS₂²⁴ and attributed to strong axial polarization along the tube axis.³³ For the largest nanotubes studied, the electron densities at conduction band and valence band exhibit clear different features between two types. This is in

consistent with previous studies that BP shows strong anisotropic electronic structure.³⁴ Structure point of view, four neighboring P atoms form a triangular pyramidal cone with a surface along zigzag direction joint together to form a larger flat plane which is very distinctive from corrugated plane along armchair direction. As a result, formation of zigzag nanotube induces larger atomic structure and thus electronic structure modification than the undulate armchair direction. This is verified by the comparison of the DOS spectra with that of monolayer BP, as given in the inset of Fig. 2(c). As shown, the DOS spectra of the armchair tubes bear great similarity to that of monolayer BP. Within 1 eV below the Fermi level (E_F), there are three major features separated into two parts. The similarity to the pristine monolayer BP indicates that the bending along armchair direction has little effect on their electronic structure. However, for the zigzag tubes, there are greatly enhanced electron states below the E_F . In later discussion, we will explain that this electronic structure change is strongly related to the valley P atoms.

On the other hand, the total DOS in Fig. 2 shows that largest energy gap for the tubes occurs in $(0, 20)$ nanotube, which is 0.79 eV under GGA. As is well known, the GGA underestimated the energy gap. For comparison purpose, the energy gap for monolayer BP was also calculated under the same condition, which is 0.68 eV. The larger band gap of nanotubes as compared to the monolayer BP is attributed to quantum confinement effect. In Fig. 2, it can be seen that for both zigzag and

armchair nanotubes the band gap is reducing with decrease of the tube diameter similar to that of MoS₂ nanotubes.²⁴ This, however, is in contrast to the quantum size effect, which indicates that structure change such as bond lengths and angles play major roles. On the other hand, for the same size tubes, armchair ones always exhibit larger energy gap. More interestingly, the energy gap of zigzag tube close for $(10, 0)$ tube. In this case, one can see from Fig. 2(f) that the conduction band and valence band merge together at E_F . But the electron states at E_F are nearly zero, which suggests the system is in a semi-metallic state. In addition, the electron states at valence band maximum (VBM) is always stronger for zigzag tubes as compared to that of armchair ones, while it is opposite for the conduction band minimum (CBM).

Unlike monolayer and bulk BP, both the $(18, 0)$ zigzag and $(0, 15)$ armchair tubes are indirect band gap as shown in Fig. 3. The VBM in both types are located at Γ points, while the CBM for the armchair tubes are located at X point which is in the middle of Γ -X line for zigzag tubes. This could be related to the zone folding, tube curvature as well as strain-dependent electronic properties.⁸ The evolution of energy gap values with respect to the tube size can be reflected from Fig. 2 for both zigzag and armchair tubes. As mentioned above, the energy gap close for $(10, 0)$ zigzag nanotubes. In addition, both of them decrease with the tube diameter nearly linearly. If the band gap values of armchair nanotubes are extrapolated to zero, the size of it would be negative which suggests that the armchair nanotubes would

always exhibit semiconducting behaviors.

In Fig. 4, the partial charge density of (18, 0) and (10, 0) nanotubes are presented to explore the origin of phase transition for zigzag nanotubes. As shown in Figs. 4(a) and (c), the CBM orbitals are mainly located at outer P atoms. However, the VBM orbitals are originated from both outer and inner P atoms with some certain periodicity along the ring. When the tube size is reduced, both CBM and VBM orbitals become more populated, see Figs. 4(c) and (d). In addition, the CBM orbitals for smaller zigzag tubes are extended to inner P atoms. This leads to enhanced orbital overlapping for the conduction and valence bands which renders the system to semi-metallic.

To explore the origin of difference between zigzag and armchair tubes, we plot the projected density of states (PDOS) for (10, 0) and (0, 10) nanotubes in Fig. 5. Due to symmetry broken after forming the nanotubes, there are two types of P atoms in the nanotube which are denoted as P1 (in the upper layer) and P3 (in the lower layer) in Fig. 1(a). After forming the tubes, P1 atoms are located in the outer ring which has larger bond length especially for the zigzag ones, see Table I. For (10, 0) zigzag nanotube where the semi-metallic states are introduced, the electronic states of P1 atoms, especially for conduction band, is much stronger than that of P3 atoms. In fact, only P1 in (10, 0) zigzag nanotube exhibits these features. In Table I, one can see that the bond length of P1 is much longer than that of P3 atoms in this case.

This indicates that the enhanced electron states near the Fermi level may be introduced by the tensile strain around the P1 atoms. As shown in Figs. 5(a) and (c), the states at CBM are dominated by P1 rather than P3 atoms. This suggests that the empty states (holes) are mainly presented in the outer ring of the zigzag tubes. This geometry distribution of the carriers is beneficial for charge separation during a photocatalytic reaction. In addition, it is seen that the s - p hybridization for the zigzag nanotubes are much stronger in the valence bands as compared to the armchair ones while it is opposite for conduction band especially for P3 atoms where the s orbitals and p_y orbitals are strongly hybridized, as shown in Fig. 5(d). From the PDOS, one learnt that for P1 atoms in zigzag nanotube, the contribution to the conduction bands is mainly from p_x orbitals, while p_x and p_z orbitals have similar contributions at VBM. In P3, conduction bands are mainly composed of p_x and p_z orbitals, while p_z , p_y and p_x orbitals contribute equally to VBM. On the other hand, for armchair nanotube, the CBM of P1 are mainly composed of p_x and p_y orbitals, while only p_x orbitals contribute to VBM. In P3, it is p_y orbitals that show strong hybridization with s orbitals and make up CBM, while p_x and p_z orbitals for VBM. In brief, the enhancement of p_z orbitals in VBM and p_x orbitals in CBM are the dominate factors for the semi-metallic state formation.

Conclusions

In summary, we studied the electronic structure of BP nanotubes. Although the band gap for both zigzag and armchair nanotubes are indirect, they exhibit strong anisotropic electronic behaviors. For zigzag nanotubes, the energy gap can close at smaller size and turn the system to a semi-metallic state. However, the armchair nanotubes always behave as semiconductor. The difference between these two configurations are correlated to their structure modification after forming the tubes where the tensile strain generated tunes the electronic behaviors. In the end, the different p orbitals distributions due to the different s - p hybridizations leads to the overall phenomena. In addition, the special distribution of charge carriers suggests that BP nanotubes may be promising candidates for photocatalytic applications.

Acknowledgements

This work was supported by Education Department of Hebei Province under the Grant No. QN2015033.

References:

- ¹ K. S. Novoselov, A. K. Geim, S. V. Morozov, D. Jiang, M. I. Katsnelson, I. V. Grigorieva, S. V. Dubonos, and A. A. Firsov, *Nature* **438**, 197 (2005).
- ² A. C. Ferrari, J. C. Meyer, V. Scardaci, C. Casiraghi, M. Lazzeri, F. Mauri, S. Piscanec, D. Jiang, K. S. Novoselov, S. Roth, and A. K. Geim, *Phys. Rev. Lett.* **97**, 187401 (2006).
- ³ A. K. Geim and K. S. Novoselov, *Nat. Mater.* **6**, 183 (2007).
- ⁴ K. S. Novoselov, A. K. Geim, S. V. Morozov, D. Jiang, Y. Zhang, S. V. Dubonos, I. V. Grigorieva, and A. A. Firsov, *Science* **306**, 666 (2004).

- 5 Q. H. Wang, K. Kalantar-Zadeh, A. Kis, J. N. Coleman, and M. S. Strano, *Nat Nano.* **7**, 699 (2012).
- 6 K. S. Novoselov, D. Jiang, F. Schedin, T. J. Booth, V. V. Khotkevich, S. V. Morozov, and A. K. Geim, *PNAS* **102**, 10451 (2005).
- 7 C. Lee, Q. Li, W. Kalb, X.-Z. Liu, H. Berger, R. W. Carpick, and J. Hone, *Science* **328**, 76 (2010).
- 8 A. S. Rodin, A. Carvalho, and A. H. Castro Neto, *Phys. Rev. Lett.* **112**, 176801 (2014).
- 9 L. K. Li, Y. J. Yu, G. J. Ye, Q. Q. Ge, X. D. Ou, H. Wu, D. L. Feng, X. H. Chen, and Y. B. Zhang, *Nat. Nanotech.* **9**, 372 (2014).
- 10 H. Liu, A. T. Neal, Z. Zhu, Z. Luo, X. Xu, D. Tománek, and P. D. Ye, *ACS Nano* **8**, 4033 (2014).
- 11 T. Jiang, H. Liu, D. Huang, S. Zhang, Y. Li, X. Gong, Y.-R. Shen, W.-T. Liu, and S. Wu, *Nat. Nanotech.* **9**, 825 (2014).
- 12 J. Qiao, X. Kong, Z.-X. Hu, F. Yang, and W. Ji, *Nat. Commun.* **5**, 4475 (2014).
- 13 Y. Deng, Z. Luo, N. J. Conrad, H. Liu, Y. Gong, S. Najmaei, P. M. Ajayan, J. Lou, X. Xu, and P. D. Ye, *ACS Nano* **8**, 8292 (2014).
- 14 M. Buscema, D. J. Groenendijk, G. A. Steele, H. S. J. van der Zant, and A. Castellanos-Gomez, *Nat. Commun.* **5**, 4651 (2014).
- 15 J.-W. Jiang, *Nanotechnology* **26**, 055701 (2015).
- 16 J.-W. Jiang and H. S. Park, *Nat. Commun.* **5**, 4727 (2014).
- 17 T. Low, M. Engel, M. Steiner, and P. Avouris, *Phys. Rev. B* **90**, 081408 (2014).
- 18 H. Wang, X. Wang, F. Xia, L. Wang, H. Jiang, Q. Xia, M. L. Chin, M. Dubey, and S.-j. Han, *Nano Lett.* **14**, 6424 (2014).
- 19 Z. Wang, H. Jia, X. Zheng, R. Yang, Z. Wang, G. J. Ye, X. H. Chen, J. Shan, and P. X. L. Feng, *Nanoscale* **7**, 877 (2015).
- 20 D. Xiang, C. Han, J. Wu, S. Zhong, Y. Liu, J. Lin, X.-A. Zhang, W. Ping Hu, B. Ozyilmaz, A. H. C. Neto, A. T. S. Wee, and W. Chen, *Nat. Commun.* **6**, 6485 (2015).
- 21 N. G. Chopra, R. J. Luyken, K. Cherrey, V. H. Crespi, M. L. Cohen, S. G. Louie, and A. Zettl, *Science* **269**, 966 (1995).
- 22 M. Myahkostupov, M. Zamkov, and F. N. Castellano, *Energy Environ. Sci.* **4**, 998 (2011).
- 23 G.-W. She, X.-H. Zhang, W.-S. Shi, X. Fan, J. C. Chang, C.-S. Lee, S.-T. Lee, and C.-H. Liu, *Appl. Phys. Lett.* **92**, 053111 (2008).
- 24 N. Li, G. Lee, Y. H. Jeong, and K. S. Kim, *J. Phys. Chem. C* **119**, 6405 (2015).
- 25 X. Peng, Q. Wei, and A. Copple, *Phys. Rev. B* **90**, 085402 (2014).
- 26 Q. Wei and X. Peng, *Appl. Phys. Lett.* **104**, 251915 (2014).

- 27 G. Seifert and E. Hernández, Chem. Phys. Lett. **318**, 355 (2000).
28 I. Cabria and J. W. Mintmire, EPL **65**, 82 (2004).
29 T. Hu, A. Hashmi, and J. Hong, Nanotechnology **26** (2015).
30 H. Kawamura, I. Shirotani, and K. Tachikawa, Solid State Commu. **49**, 879
(1984).
31 P. E. Blöchl, Phys. Rev. B **50**, 17953 (1994).
32 J. P. Perdew, K. Burke, and M. Ernzerhof, Phys. Rev. Lett. **77**, 3865 (1996).
33 V. V. Gobre and A. Tkatchenko, Nat. Commun. **4**, 2341 (2013).
34 R. Fei and L. Yang, Nano Lett. **14**, 2884 (2014).

Table I. Structure information for both types of black phosphorus nanotubes

	Diameter (Å)	Bond length (Å)		Bond angle (°)	
		Lower (P3)	Upper (P1)	Lower (P3)	Upper (P1)
Monolayer		2.22	2.22	95.9	95.9
		Zigzag			
(10, 0)	15	2.18	2.52	91.9	119.3
(18, 0)	23	2.19	2.41	92.8	107.2
(25, 0)	30	2.21	2.37	94.3	104.8
		Armchair			
(0, 10)	18	2.21	2.24	97.1	94.9
(0, 15)	26	2.21	2.24	96.8	95.2
(0, 20)	33	2.21	2.24	96.9	95.4

Figure captions:

Fig. 1. (Color online) (a) Ball-and-stick model for phosphorene. The zigzag and armchair directions are indicated. Position of P1 and P3 atoms are denoted. (b) naming scheme for zigzag and armchair nanotubes. Side and top view of armchair (c) and zigzag (d) nanotubes.

Fig. 2. (Color online) Density of state (DOS) spectra for the chosen nanotubes. (a)-(c) are that for $(0, 20)$, $(0, 15)$ and $(0, 10)$ armchair nanotubes with diameters of 33 Å, 26 Å, and 18 Å, respectively. (d)-(f) are that for $(10, 0)$, $(18, 0)$ and $(25, 0)$ zigzag nanotubes with diameters of 30 Å, 23 Å, and 15 Å, respectively. The inset in (c) are the DOS for monolayer BP. The fermi energy is set to 0 eV.

Fig. 3. (Color online) Band structure representative for $(18,0)$ zigzag (a) and $(0,15)$ armchair (b) nanotubes. The fermi energy is set to 0 eV.

Fig. 4. (Color online) Partial charge density distribution at Γ point. (a) and (b) are CBM and VBM for zigzag $(18, 0)$ nanotube; (c) and (d) are that of zigzag $(10, 0)$ nanotube. The top (side) views for all cases are given on the left (right). The isosurface value is set to $0.001 \text{ e}/\text{\AA}^3$.

Fig. 5. (Color online) Project density of state (PDOS) spectra for the chosen nanotubes. (a) and (b) are that for P1 and P3 in $(10, 0)$ zigzag nanotubes, respectively. (c) and (d) are that for P1 and P3 in $(0, 10)$ armchair nanotube, respectively. The orbital decomposed spectra are recognized by their different color as indicated in (b). The fermi energy is set to 0 eV.

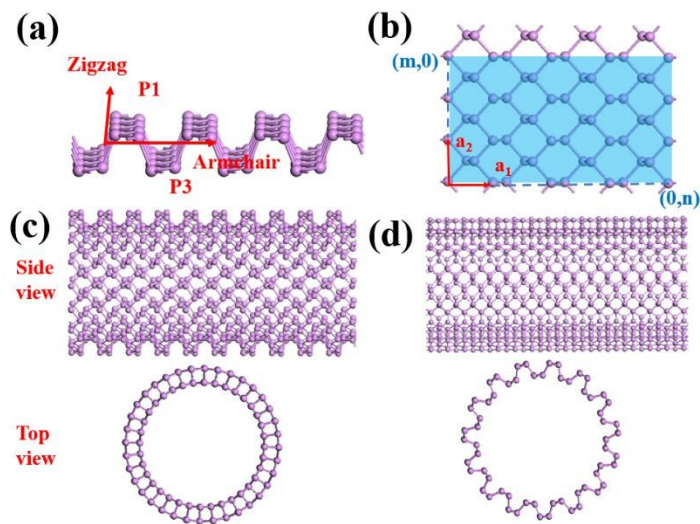


Fig. 1 Guan et al.

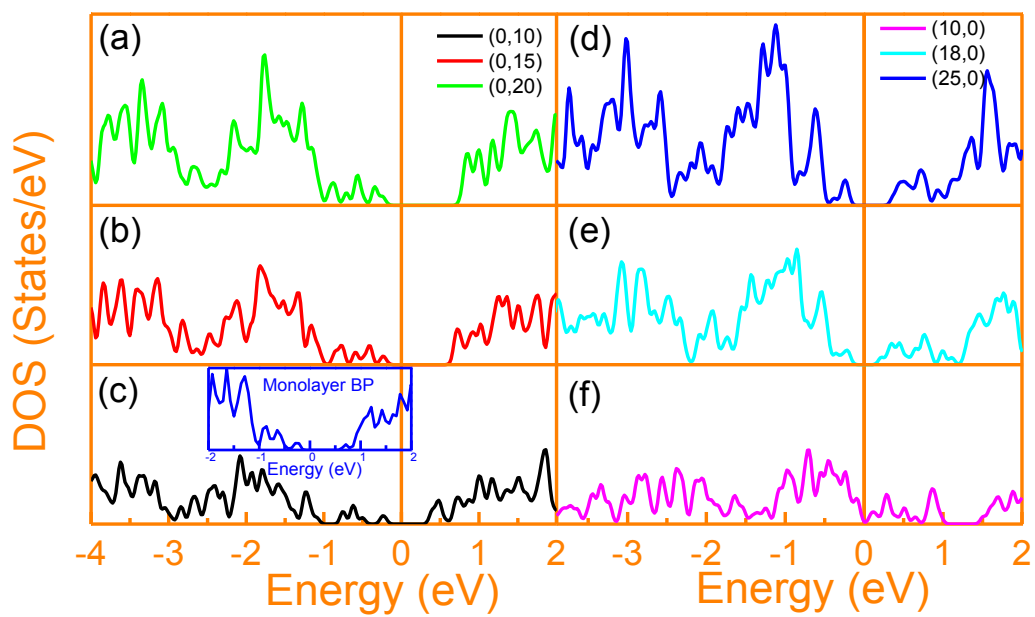


Fig. 2 Guan et al.

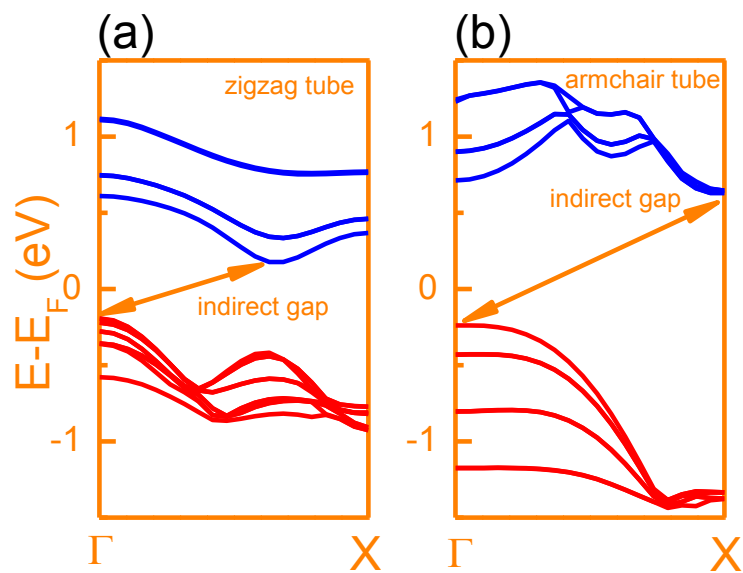


Fig. 3 Guan et al.

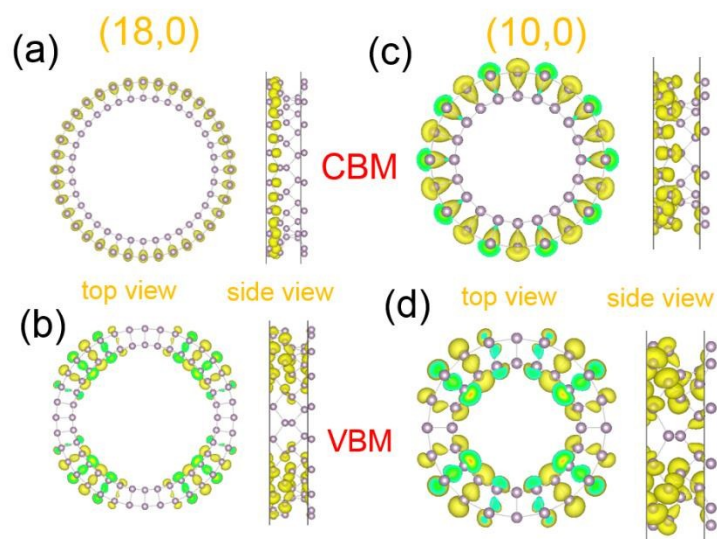


Fig. 4 Guan et al.

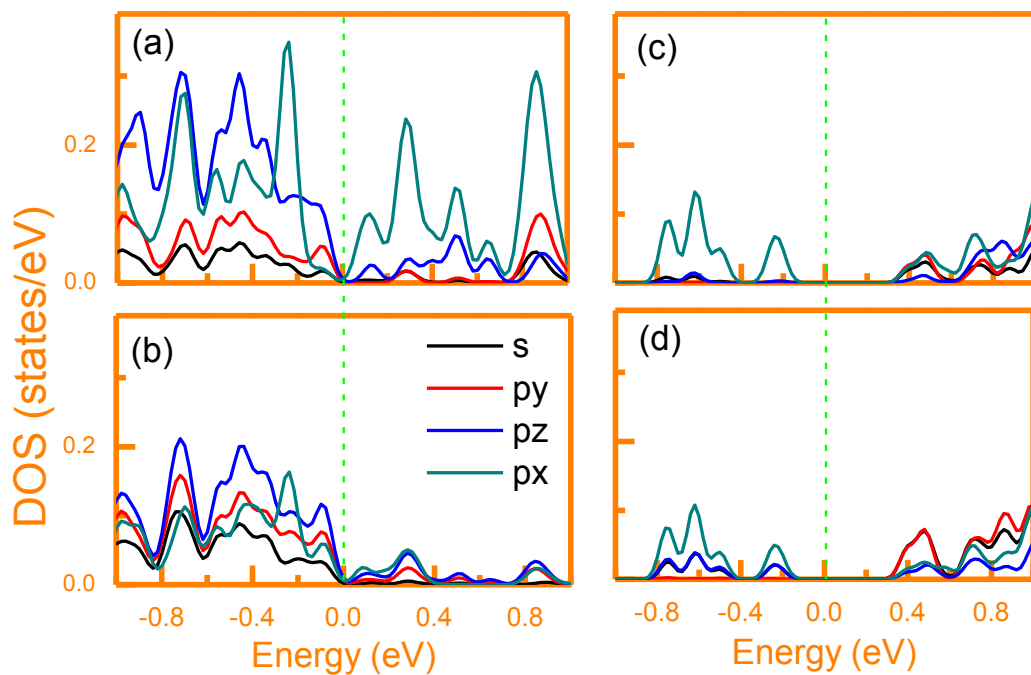


Fig. 5 Guan et al.